Archives of Academic Emergency Medicine. 2024; 12(1): e31

OPEN ACCESS

ORIGINAL RESEARCH

Hypo-attenuating Berry Sign as a Novel Imaging Marker of Ruptured Aneurysm in Patients with Subarachnoid Hemorrhage; a Diagnostic Accuracy Study

Xin-Wei Zhou[&1,2], Shu-Feng Cai[&3], De-Qing Zhang[3], Gang Xiao[4], Jing Liu[5], Wen-Jie Yang[6], Yi Li[3], Si-Yu Chen[7], Hao-Chen Liu[7], Zhong-Qing Huang[3]*

1. Medical Research Center, Yuebei People's Hospital, Shantou University Medical College, Shaoguan, Guangdong Province, China
2. Department of Ultrasound, Yuebei People's Hospital, Shantou University Medical College, Shaoguan, Guangdong Province, China
3. Department of Medical Image Center, Yuebei People's Hospital, ShantouUniversity Medical College, Shaoguan, Guangdong Province, China
4. Department of Neurosurgery, Yuebei people's Hospital, Shantou University Medical College, Shaoguan, Guangdong Province, China
5. Administrative Office, Yuebei people's Hospital, Shantou University Medical College, Shaoguan, Guangdong Province, China
6. Department of Diagnostic Radiology and Nuclear Medicine, University of Maryland, Baltimore, MD, the USA
7. The First Clinical Medical College, Guangdong medical university, Zhanjiang Province, China

Received: December 2023; Accepted: January 2024; Published online: 26 February 2024

Abstract: **Introduction:** Aneurysmal subarachnoid hemorrhage (SAH) constitutes a life-threatening condition, and identifying the ruptured aneurysm is essential for further therapy. This study aimed to evaluate the diagnostic accuracy of hypo-attenuating berry sign (HBS) observed on computed tomography (CT) scan in distinguishing ruptured aneurysms. **Methods:** In this diagnostic accuracy study, patients who had SAH and underwent non-enhanced brain CT scan were recruited. The HBS was defined as a hypo-attenuating area with an identifiable border in the blood-filled hyper-dense subarachnoid space. The screening performance characteristics of HBS in identifying ruptured aneurysms were calculated considering the digital subtraction angiography (DSA) as the gold standard. **Results:** A total of 129 aneurysms in 131 patients were analyzed. The overall sensitivity and specificity of HBS in the diagnosis of aneurysms were determined to be 78.7% (95%CI: 73.1% - 83.4%) and 70.7% (95%CI: 54.3% - 83.4%), respectively. Notably, the sensitivity increased to 90.9% (95%CI: 84.3% - 95.0%) for aneurysms larger than 5mm. The level of inter-observer agreement for assessing the presence of HBS was found to be substantial (kappa=0.734). The diagnostic accuracy of HBS in individuals exhibited enhanced specificity, sensitivity, and reliability when evaluating patients with a solitary aneurysm or assessing ruptured aneurysms. The multivariate logistic regression analysis revealed a statistically significant relationship between aneurysm size and the presence of HBS (odds ratios of 1.667 (95%CI: 1.238 - 2.244; $p < 0.001$) and 1.696 (95%CI: 1.231 - 2.335; $p = 0.001$) for reader 1 and reader 2, respectively). **Conclusion:** The HBS can serve as a simple and easy-to-use indicator for identifying a ruptured aneurysm and estimating its size in SAH patients.

Keywords: Subarachnoid hemorrhage; Intracranial aneurysm; Angiography; Artificial intelligence; Retrospective studies; Tomography, X-ray computed

Cite this article as: Zhou X-W, Cai S-F, Zhang D-Q, et al. Hypo-attenuating Berry Sign as a Novel Imaging Marker of Ruptured Aneurysm in Patients with Subarachnoid Hemorrhage; a Diagnostic Accuracy Study. Arch Acad Emerg Med. 2024; 12(1): e31. https://doi.org/10.22037/aaem.v12i1.2154.

1. Introduction

Subarachnoid hemorrhage (SAH) is the third most common subtype of stroke, and the rupture of an intracranial aneurysm is the most common cause of SAH (1, 2). Given the high morbidity and mortality of patients with aneurysmal SAH (1, 3), prompt detection, accurate localization, and evaluation of the aneurysm are critical for determining the appropriate endovascular or neurosurgical therapy (4-6).

However, identifying the site of ruptured aneurysms based solely on clinical symptoms may lead to misdiagnosis or missed diagnosis because clinical presentations of aneurysmal SAH are non-specific, varying from acute onset of severe headache with or without focal neurological deficits to ongoing or severe loss of consciousness, depending on the extent of bleeding (1, 3, 7, 8). Digital subtraction angiography (DSA) serves as the standard technique for evaluating intracranial

***Corresponding Author:** Zhong-Qing Huang, 133 Huiming road, Yuebei People's Hospital, Guangdong Province, China, 512026. Email: hzq5964296@sina.com, Tel: +86 17817262875, ORCID: https://orcid.org/0000-0002-6623-5959.

&Both authors contributed equally to this manuscript.

aneurysms, but it is invasive and associated with a 0.5% risk of permanent neurologic complications (4).

Computed tomography (CT) scan is a routine clinical imaging for patients with suspected SAH because of its high sensitivity and wide availability for rapid diagnosis. In patients presenting with a single aneurysm, the determination of the aneurysm's location through the analysis of SAH distribution type on non-enhanced CT (NECT) scan is successful in only a range of 59% to 80% of cases (6, 9-11).

Besides, in instances where multiple aneurysms are present, the identification of the specific ruptured aneurysm on NECT may be susceptible to misinterpretation, resulting in postoperative rebleeding (7, 8). Furthermore, the precise location of a ruptured aneurysm is of great importance to the neurosurgeons because the rapidly increasing use of endovascular coiling may be associated with greater uncertainty that the ruptured aneurysm has been treated in patients with multiple aneurysms (9, 12). In the cohort of patients diagnosed with aneurysmal SAH, we have observed the presence of a hypo-attenuating area within the hyper-dense subarachnoid space filled with blood on NECT, which we have designated as HBS. We believe that this radiological sign holds promise as a novel imaging marker for the identification of ruptured aneurysm and the estimation of aneurysm size. Consequently, this study aimed to report findings on the utility of this radiological indicator in discerning ruptured aneurysms and estimating aneurysm size.

2. Methods

2.1. Study design and setting

For this diagnostic accuracy study, patients who had SAH and underwent non-enhanced brain CT (NECT) scan at Yuebei People's Hospital, ShaoguanUniversity Medical College, China, between December 2021 and January 2023, were selected as participants in the test group. The screening performance characteristics of HBS in identifying ruptured aneurysms were calculated considering the DSA as the gold standard. This study was approved by the institutional Ethics committee (Ethics code: YBEC-KY(2023)-029 and YBEC-KY(2024)-004) and written informed consent was exempted due to the study design entailing no diagnostic tests or treatment.

2.2. Participants

A total of 1137 patients were identified from the electronic health record system using the search keyword "SAH". Inclusion criteria for the study group were the following: 1) patients with SAH; 2) first NECT performed ≤ 72 h after symptom onset (Time interval is of special interest(1,9)); and 3) at least had one angiography exam after the onset of SAH to confirm the ruptured aneurysm. Exclusion criteria were the following: 1) enhanced scan within 48 h for other purposes of imaging study before symptom onset; 2) NECT only acquired at outside hospital; 3) insufficient image quality to evaluate SAH or incomplete clinical records in the electronic health record system; 4) SAH related to brain tumor, traumatic brain injury, arteriovenous malformation, arteriovenous fistula, moyamoya disease, or hemorrhagic infarction; and 5) fusiform aneurysm or aneurysm size < 3 mm.

2.3. Data gathering

Clinical and demographic characteristics, including sex, age, time interval between NECT and symptom onset, underlying disease (diabetes mellitus, hypertension, hyperlipidemia), and clinical severity scores of SAH (Hunt-Hess score), were collected from the electronic health record system at our hospital. Imaging findings (presence of HBS, aneurysm size and location, attenuation value on Hounsfield unit, etc.) were recorded by the researchers (The Fisher score and imaging findings were not obtained from the electronic health record system; instead, they were documented by the researchers).

The HBS on NECT was defined as 1) A relatively isolated hypo-attenuating area in the blood-filled hyper-dense subarachnoid space; 2) The hypodense region can be round, oval, or berry-shaped with an identifiable border; 3) Less than 1/5 length of circumference of hypo-attenuating area is connected with the adjacent brain tissue; 4) The average attenuation value (Hounsfield Units = HU) of the hypo-attenuating region should be higher than that of cerebrospinal fluid but lower than adjacent SAH (Figure 1).

2.4. Image acquisition

All patients underwent head NECT scans using a 64-channel multi-detector CT scanner (LightSpeed VCT, GE Medical Systems, USA, and uCT 760, United Imaging, China). A routine NECT protocol was performed using a collimation of 20×0.625 mm, a tube voltage of 120 kV, a tube current of 240-350 mAs, and a reconstruction interval of 0.625 mm with a "standard" algorithm. All NECT images were rebuilt into 3 spatial directions (coronal, sagittal, and transverse) with 2.5mm thickness using multi-planar reformation on the workstation that came with the CT scanner. The CT angiography and DSA used in this study have previously been described in the literature (13, 14).

2.5. Image analysis and interpretation

A total of 29 patients with confirmed aneurysmal SAH were recruited in the training group, and each patient's data was independently analyzed by four radiologists/readers. The readers were blinded to the clinical characteristics of the patients and underwent a training protocol that involved 3 steps. In step 1, readers independently evaluated the allocation of the subarachnoid blood on NECT to identify the location of ruptured aneurysm, which was categorized as anterior and posterior circulation. In step 2, DSA was considered as the standard of reference and analyzed in consensus by the readers. After comparing results based on NECT and angiography, readers re-evaluated the misdiagnosed or missed diagnosis images in consensus. Readers repeated steps 1 and

2 if the diagnostic accuracy of aneurysm location was less than 90%. In step 3, the training was subjected to individual review by readers to detect the presence of HBS. In order to ensure reliability, readers evaluated the images in consensus and re-analyzed step 3 if the intra-class correlation coefficient (ICC) fell below 0.75.

The training group analysis was performed more than three months before the test group analysis, to avoid recall biases. The NECT images within the study group were de-identified and allocated to Readers 1 and 2, both of whom possessed 12 years of professional experience, for the purpose of conducting independent analysis. These readers were unaware of the angiographic images and the clinical characteristics associated with the images. The presence of HBS was assessed using a 5-point scale: 1, definitely absent; 2, possibly absent; 3, equivocal; 4, possibly present; and 5, definitely present. In cases where HBS was deemed definitely or possibly present, the location and the size of HBS were recorded, along with the attenuation value of SAH surrounding HBS (with a region of interest size set at 10-15 mm2). For individuals with an assessment score of 3 or lower, the region with the highest SAH density was chosen to measure the attenuation value. Readers documented the Fisher core for all cases.

Angiography was reviewed by a neurosurgeon (reader 3), with 12 years of working experience, who was blinded to the NECT analysis.

Aneurysm size, location, and status (ruptured or unruptured) were recorded. The locations of aneurysms in the study group were categorized into four sites (14, 15): 1) internal carotid artery (ICA), including ICA terminus, posterior communicating artery, and cavernous ICA; 2) middle cerebral artery (MCA), including the M1–2 bifurcations; 3) anterior cerebral artery (ACA) including anterior communicating artery; and 4) posterior circulation artery, including vertebral artery and posterior cerebral artery. The determination of the size of the aneurysm in each patient was conducted by assessing its greatest dimension. All measurements were performed on workstations equipped with an electronic caliper at a magnification of ×4(14). Patients with SAH underwent one follow-up angiography for clinical purposes if the initial imaging exam(s) were negative for detecting an aneurysm (It was the standard protocol of hospital).

2.6. Statistical analyses

All data were analyzed using SPSS 26.0 (Chicago, IL, USA). Quantitative variables were presented as mean ± standard deviation, and categorical data were presented as numbers (percentage). The sensitivity, specificity, positive predictive value, and negative predictive value of the HBS in identifying aneurysms were calculated using DSA as the gold standard reference. Univariate analysis was performed using chi-square or Fisher's exact test, and independent samples t-test as appropriate. Multivariate logistic regression model using an enter method was utilized to yield the odds ratio (OR) and 95% confidence interval (CI) for independent contributors associated with the presence of HBS. The Hosmer-Lemeshow test was used to evaluate the fitness of the logistic regression model. Furthermore, inter-observer agreement of quantitative variables was assessed using the ICC with a two-way random-effects model with absolute measurements, and categorical variables were analyzed using Cohen's kappa.

3. Results

3.1. Baseline characteristics of studied cases

A total of 131 SAH patients with the mean age of 61.8 ± 10.9 (range: 28 - 88) years (61.8% female) were enrolled in the study (Figure 2). 99 (75.6%) cases were diagnosed with hypertension, 17 (12.9%) cases had diabetes, 9 (6.9%) cases had hyperlipidemia, and 7 (5.3%) cases had a history of smoking. The time interval between symptom onset and performing non-contrast CT scan was 10.2 ± 16.6 hours. 129 aneurysms were identified in the studied cases, and 14 (10.7%) patients had multiple aneurysms (12 had 2 aneurysms, 2 had 3 aneurysms). 32 (24.8%) aneurysms were located in the ACA, 23 (17.8%) at the MCA, 57 (44.2%) at the ICA, and 17 (13.2%) in the posterior circulation arteries. Table 1 shows the clinical severity of SAHs based on Hunt-Hess and Fisher scores.

3.2. HBS frequency and characteristics

HBS was observed on NECT scan of 71.9% of cases. Table 2 compares the baseline characteristics between cases with and without HBS. The overall mean size of aneurysm measured on DSA was significantly larger for aneurysms exhibiting the HBS compared to those without the HBS (6.7±3.2 mm versus 4.4±1.6 mm, $p < 0.001$). Furthermore, in the case of true positive aneurysms, the size determined through NECT was found to be larger compared to the size measured using DSA (7.6 ± 3.4 mm vs. 6.7 ± 3.2mm, $R = 0.840$, $p < 0.001$ for reader 1; 6.8 ± 3.0 mm vs. 6.7 ± 3.2mm, $R = 0.753$, $p < 0.001$ for reader 2). The level of agreement between the two readers regarding the size of aneurysms was found to be substantial (ICC=0.796) in cases where both readers diagnosed true positive aneurysms. The HBS positive group exhibited significantly increased overall Hunt-Hess score ($p<0.001$) and Fisher score ($p<0.001$), higher prevalence of diabetes mellitus ($p <0.01$), and higher attenuation value of SAH ($p < 0.05$) compared to patients without HBS. However, the size of the aneurysm was the only significant predictor of HBS presence on multivariate analysis (Table 3).

3.3. Screening performance characteristics of HBS

Table 4 presents the sensitivity, specificity, positive predictive value (PPV), and negative predictive value (NPV) of HBS in detection of ruptured aneurysms in patients with SAH. The overall sensitivity and specificity of HBS in diagnosis of aneurysms were determined to be 78.7% (95%CI: 73.1% - 83.4%) and 70.7% (95%CI: 54.3% - 83.4%), respectively. Notably, the sensitivity increased to 90.9% (95%CI:

84.3% - 95.0%) for aneurysms larger than 5mm in size. The level of inter-observer agreement for assessing the presence of HBS was found to be substantial (kappa=0.734), while the inter-observer agreement for aneurysm size more than 5mm was determined to be excellent (kappa=1.000). The study assessed the diagnostic performance of HBS in patients with a solitary aneurysm, yielding an overall sensitivity of 86.4% (95%CI: 80.6% - 90.7%) and specificity of 74.4% (95%CI: 57.6% - 86.4%). Additionally, substantial inter-observer agreement was observed between reader 1 and reader 2, as indicated by a kappa value of 0.766. When examining ruptured aneurysm, HBS demonstrated an overall sensitivity of 87.4% (95%CI: 82.1% - 91.3%) and specificity of 80.6% (95%CI: 63.4% - 91.2%), with substantial inter-observer agreement between readers (kappa=0.772).

4. Discussion

This study presents empirical evidence supporting the utilization of the HBS on NECT as a novel marker for the detection of aneurysms in patients with SAH. The findings indicate that this marker exhibits enhanced sensitivity and specificity in diagnosing ruptured aneurysms with a diameter > 5mm or in patients presenting with a single ruptured aneurysm. Furthermore, the size of the aneurysm is identified as an independent factor influencing the manifestation of HBS in an individual.

The SAH pattern on NECT is a typical but challenging sign for distinguishing ruptured aneurysms (10, 16-19). The sensitivity of the SAH pattern in localizing the site of aneurysm rupture varies from 45%(17) to 100%(18), along with inter-reader agreement that varies from 0.4(16, 18) to 0.9(10). The findings of our study demonstrate that the utilization of HBS can yield a high level of sensitivity and specificity in identifying the site of a ruptured aneurysm. Furthermore, when focusing on aneurysms larger than 5mm or patients with a single aneurysm, the sensitivity, specificity, and reliability of HBS are further augmented. In such conditions, the combined sensitivity can potentially reach up to 90.9% (95%CI: 84.3% - 95.0%), while the specificity can reach up to 74.4% (95%CI: 57.6% - 86.4%). In emergency scenarios involving patients with SAH, emergency physicians anticipate the utilization of NECT to ascertain the precise origin of hemorrhage with utmost accuracy.

Consequently, the metrics of sensitivity and specificity for each ruptured aneurysm are of great academic interest. Our study's findings revealed an overall sensitivity of 87.9% and specificity of 80.6% per ruptured aneurysm, accompanied by substantial inter-observer agreement. Previous studies had revealed that SAH pattern demonstrated potential for predicting ruptured ACA (16) or MCA (10) aneurysms, but, it was deemed unreliable for locating ruptured posterior circulation aneurysms (10, 16, 19). Nevertheless, our study did not find any notable disparities in location when considering the diagnostic value of HBS. To elucidate this phenomenon, various factors should be taken into account. These factors encompass the atypical distribution of SAH caused by the blood jet to spread in many different directions (19, 20) and the presence of adhesions in the subarachnoid cisterns resulting from a previous minor leakage (8, 20). Regardless of the leakage process and direction of the blood jet into the cisterns, it can be hypothesized that the blood would initially accumulate around the ruptured aneurysm, thereby facilitating the presence of HBS. Therefore, it is plausible that HBS may be more advantageous than the SAH pattern when it comes to localizing aneurysms in the posterior circulation. Other traditional imaging signs, such as hematoma (10, 16, 19) and focal mass effect (10, 17) on NECT, were found to be highly reliable but had a relatively low occurrence rate (approximately 15%) in indicating the site of rupture.

Conversely, the occurrence of hydrocephalus and intraventricular hemorrhage is not low (1, 21), yet their reliability is notably insufficient (17, 21, 22). It is noteworthy to acknowledge that, apart from the aforementioned robust reliability of HBS in identifying ruptured aneurysms, the collective prevalence of HBS was determined to be 71.9%. The utilization of all accessible indicators to determine the location of the ruptured aneurysm is crucial within the realm of routine clinical practice.

DSA can provide absolute proof of the ruptured aneurysm using a smoking gun sign (contrast media extravasation), but smoking gun sign is rarely observed (23, 24). Additional signs gained by using NECT would therefore be of great value for patients with multiple aneurysms. In the univariate analysis, it was found that the Hunt-Hess score and the Fisher score were significantly higher in the HBS positive group compared to the negative group. However, in the multivariate analysis, these scores did not exhibit a statistically significant difference. These findings are consistent with a previous study which indicated that the total amount of hemorrhage does not impact the diagnosis of the site of the ruptured aneurysm (10). The multivariate logistic regression analysis only revealed a statistically significant relationship between aneurysm size and the occurrence of HBS (Overall OR (95%CI) = 1.669(1.345-2.070)), indicating that the HBS is more accurate in identifying larger aneurysms. Moreover, for true positive aneurysm, the measurement of aneurysm size on NECT was found to be significantly consistent with that on DSA.

However, HBS tended to result in a slight overestimation of the aneurysm size when compared to DSA. The exact reason is unclear, though we suspect partial volume effect and aneurysm wall thickness may be responsible for the phenomenon. The assessment conducted using NECT included measurements of the aneurysm wall thickness, whereas the assessment conducted using DSA solely encompassed measurements of the internal diameter of the aneurysm, excluding the wall thickness. Theoretically, the attenuation value of the space surrounding an un-ruptured aneurysm is equivalent to that of cerebrospinal fluid. However, in the case of a ruptured aneurysm, the surrounding space is filled with

the mixture of cerebrospinal fluid and freshly extravasated blood, and subsequently, the attenuation value of surrounding space increases (9), which may be similar to the attenuation value of aneurysm wall (22). In addition, including surrounding space resulted in the excessive measurement of the aneurysm.
CT angiography is partially omitted in patients with aneurysmal SAH in our center, if hybrid operation room is available in an emergency setting, because the probability of NECT finding the ruptured aneurysm is relatively high and DSA is usually performed right after the NECT scan. Radiation exposure (25, 26), contrast agent administration, and treatment waiting time are minimized, thereby patient care process is potentially improved and the burden on medical resources is reduced. A previous study has demonstrated the safety and accuracy of endovascular aneurysm repair without the need for pre-and intra-operative contrast agents (27). Recent researches have established the effectiveness of artificial intelligence in the pretreatment evaluation of intracranial hemorrhage (28) and aortic dissection (29) based on NECT.
We think the utilization of HBS as a bio-marker presents a promising avenue for training artificial intelligence algorithms in the detection of ruptured aneurysms using NECT. Our group intends to deliver a forthcoming report on the assessment of NECT-based artificial intelligence for the pretreatment evaluation of intracranial aneurysms.

5. Limitations

First, a limited number of subjects were recruited in this study, and a retrospective analysis could cause biased selection of participants. Second, prior to analyzing the study group, the readers who took part in the study underwent comprehensive training and were provided with reinforcement of the established rules. Our skepticism arises from the notion that the efficacy of HBS in diagnosing aneurysms is influenced by adherence to the training protocol. Consequently, it is plausible that supplementary training may be necessary for the successful implementation of HBS detection in clinical practice for the identification of aneurysms. Third, the evaluation of HBS is not completely objective.
Finally, we did not set an attenuation threshold for HBS. The average value of hypo-attenuating region was 42.5 (range, 27-59) HU. Further research is needed to determine the optimal HU threshold of HBS in order to test its sensitivity and specificity in diagnosing aneurysms.

6. Conclusions

The HBS holds promise as an imaging marker for accurate and timely detection of ruptured aneurysms and estimation of their size in patients with aneurysmal SAH.

7. Declarations

7.1. Acknowledgments

None.

7.2. Using artificial intelligence chatbots

None.

7.3. Non-standard Abbreviations and Acronyms

SAH: subarachnoid hemorrhage; ICA: internal carotid artery; MCA: middle cerebral artery; ACA: anterior cerebral artery; DSA: digital subtraction angiography; CT: computed tomography; NECT: non-enhanced CT; HBS: hypo-attenuating berry sign; HU: Hounsfield unit; ICC: intraclass correlation coefficient; OR: odds ratio; CI: confidence interval; PPV: positive predictive value; NPV: negative predictive value.

7.4. Conflict of interest

The authors declare that they have no conflicts of interest.

7.5. Funding and support

No funding source to declare. The scientific guarantor of this publication is Zhongqing Huang.

7.6. Author contributions

Conception and design: Xin-Wei Zhou, Zhong-Qing Huang.
Clinical data collection and image review: Xin-Wei Zhou, Shu-Feng Cai, De-Qing Zhang, Gang Xiao, Yi Li, Si-Yu Chen, Hao-Chen Liu, Zhong-Qing Huang.
Statistical analysis and interpretation of the data: Xin-Wei Zhou, Jing Liu, Wen-Jie Yang.
Drafting of the article: Xin-Wei Zhou, Shu-Feng Cai.
Critical revision of the article for important intellectual content: Jing Liu, Wen-Jie Yang.
All authors read and approved final version of manuscript.

References

1. Macdonald RL, Schweizer TA. Spontaneous subarachnoid haemorrhage. Lancet. 2017;389(10069):655-66.
2. Claassen J, Park S. Spontaneous subarachnoid haemorrhage. Lancet. 2022;400(10355):846-62.
3. Connolly ES, Jr., Rabinstein AA, Carhuapoma JR, Derdeyn CP, Dion J, Higashida RT, et al. Guidelines for the management of aneurysmal subarachnoid hemorrhage: a guideline for healthcare professionals from the American Heart Association/american Stroke Association. Stroke. 2012;43(6):1711-37.
4. Cloft HJ, Joseph GJ, Dion JE. Risk of cerebral angiography in patients with subarachnoid hemorrhage, cerebral aneurysm, and arteriovenous malformation: a meta-analysis. Stroke. 1999;30(2):317-20.
5. Lubicz B, Levivier M, Francois O, Thoma P, Sadeghi N, Collignon L, et al. Sixty-four-row multisection CT angiography for detection and evaluation of ruptured intracra-

nial aneurysms: interobserver and intertechnique reproducibility. AJNR Am J Neuroradiol. 2007;28(10):1949-55.

6. Hillman J. Selective angiography for early aneurysm detection in acute subarachnoid haemorrhage. Acta Neurochir (Wien). 1993;121(1-2):20-5.
7. Hino A, Fujimoto M, Iwamoto Y, Yamaki T, Katsumori T. False localization of rupture site in patients with multiple cerebral aneurysms and subarachnoid hemorrhage. Neurosurgery. 2000;46(4):825-30.
8. Lee KC, Joo JY, Lee KS. False localization of rupture by computed tomography in bilateral internal carotid artery aneurysms. Surg Neurol. 1996;45(5):435-40; discussion 40-1.
9. Liliequist B, Lindqvist M, Valdimarsson E. Computed tomography and subarachnoid hemorrhage. Neuroradiology. 1977;14(1):21-6.
10. Karttunen AI, Jartti PH, Ukkola VA, Sajanti J, Haapea M. Value of the quantity and distribution of subarachnoid haemorrhage on CT in the localization of a ruptured cerebral aneurysm. Acta Neurochir (Wien). 2003;145(8):655-61; discussion 61.
11. Latchaw RE, Silva P, Falcone SF. The role of CT following aneurysmal rupture. Neuroimaging Clin N Am. 1997;7(4):693-708.
12. Vajda J, Juhasz J, Orosz E, Pasztor E, Toth S, Horvath M. Surgical treatment of multiple intracranial aneurysms. Acta Neurochir (Wien). 1986;82(1-2):14-23.
13. Huang ZQ, Zhou XW, Hou ZJ, Huang SQ, Meng ZH, Wang XL, et al. Risk factors analysis of mirror aneurysms: A multi-center retrospective study based on clinical and demographic profile of patients. Eur J Radiol. 2017;96:80-4.
14. Huang ZQ, Meng ZH, Hou ZJ, Huang SQ, Chen JN, Yu H, et al. Geometric Parameter Analysis of Ruptured and Unruptured Aneurysms in Patients with Symmetric Bilateral Intracranial Aneurysms: A Multicenter CT Angiography Study. AJNR Am J Neuroradiol. 2016;37(8):1413-7.
15. Backes D, Vergouwen MD, Velthuis BK, van der Schaaf IC, Bor AS, Algra A, et al. Difference in aneurysm characteristics between ruptured and unruptured aneurysms in patients with multiple intracranial aneurysms. Stroke. 2014;45(5):1299-303.
16. van der Jagt M, Hasan D, Bijvoet HW, Pieterman H, Dippel DW, Vermeij FH, et al. Validity of prediction of the site of ruptured intracranial aneurysms with CT. Neurology. 1999;52(1):34-9.
17. Nehls DG, Flom RA, Carter LP, Spetzler RF. Multiple intracranial aneurysms: determining the site of rupture. J Neurosurg. 1985;63(3):342-8.
18. Slonimsky E, Upham K, Pepley S, Ouyang T, King T, Fiorelli M, et al. Multiplanar CT evaluation of aneurysm rupture signs in subarachnoid hemorrhage. Emerg Radiol. 2022;29(3):427-35.
19. Sawicki M, Kosciukiewicz K, Jezewski D, Chelstowski K, Golofit P, Skoczylas MM, et al. Diagnostic value of non-enhanced computed tomography in identifying location of ruptured cerebral aneurysm in patients with aneurysmal subarachnoid haemorrhage. Neurol Neurochir Pol. 2020;54(1):47-53.
20. Takeuchi S, Takasato Y, Masaoka H, Hayakawa T, Otani N, Yoshino Y, et al. [Unusual distribution of blood in a ruptured aneurysm–case report]. Brain Nerve. 2009;61(12):1425-8.
21. Kayama T, Sugawara T, Sakurai Y, Ogawa A, Onuma T, Yoshimoto T. Early CT features of ruptured cerebral aneurysms of the posterior cranial fossa. Acta Neurochir (Wien). 1991;108(1-2):34-9.
22. Tryfonidis M, Evans AL, Coley SC, Hodgson TL, Connolly DJ, Romanowski CA, et al. The value of radio-anatomical features on non-contrast CT scans in localizing the source in aneurysmal subarachnoid haemorrhage. Clin Anat. 2007;20(6):618-23.
23. Jamieson KG. Rupture of an intracranial aneurysm during cerebral angiography. J Neurosurg. 1954;11(6):625-8.
24. Waga S, Kondo A, Moritake K, Handa H. Rupture of intracranial aneurysm during angiography. Neuroradiology. 1973;5(3):169-73.
25. Huang ZQ, Yang WJ, Xiao G, Yang Z, Yu H, Wu JW, et al. Characteristics of Radiation-Related Intracranial Aneurysms: A Multicenter Retrospective Study. AJNR Am J Neuroradiol. 2022;43(8):1131-5.
26. Alons IME, Goudsmit BFJ, Jellema K, van Walderveen MAA, Wermer MJH, Algra A. Yield of Computed Tomography (CT) Angiography in Patients with Acute Headache, Normal Neurological Examination, and Normal Non Contrast CT: A Meta-Analysis. J Stroke Cerebrovasc Dis. 2018;27(4):1077-84.
27. Kaladji A, Dumenil A, Mahe G, Castro M, Cardon A, Lucas A, et al. Safety and accuracy of endovascular aneurysm repair without pre-operative and intra-operative contrast agent. Eur J Vasc Endovasc Surg. 2015;49(3):255-61.
28. Kaka H, Zhang E, Khan N. Artificial Intelligence and Deep Learning in Neuroradiology: Exploring the New Frontier. Can Assoc Radiol J. 2021;72(1):35-44.
29. Hata A, Yanagawa M, Yamagata K, Suzuki Y, Kido S, Kawata A, et al. Deep learning algorithm for detection of aortic dissection on non-contrast-enhanced CT. Eur Radiol. 2021;31(2):1151-9.

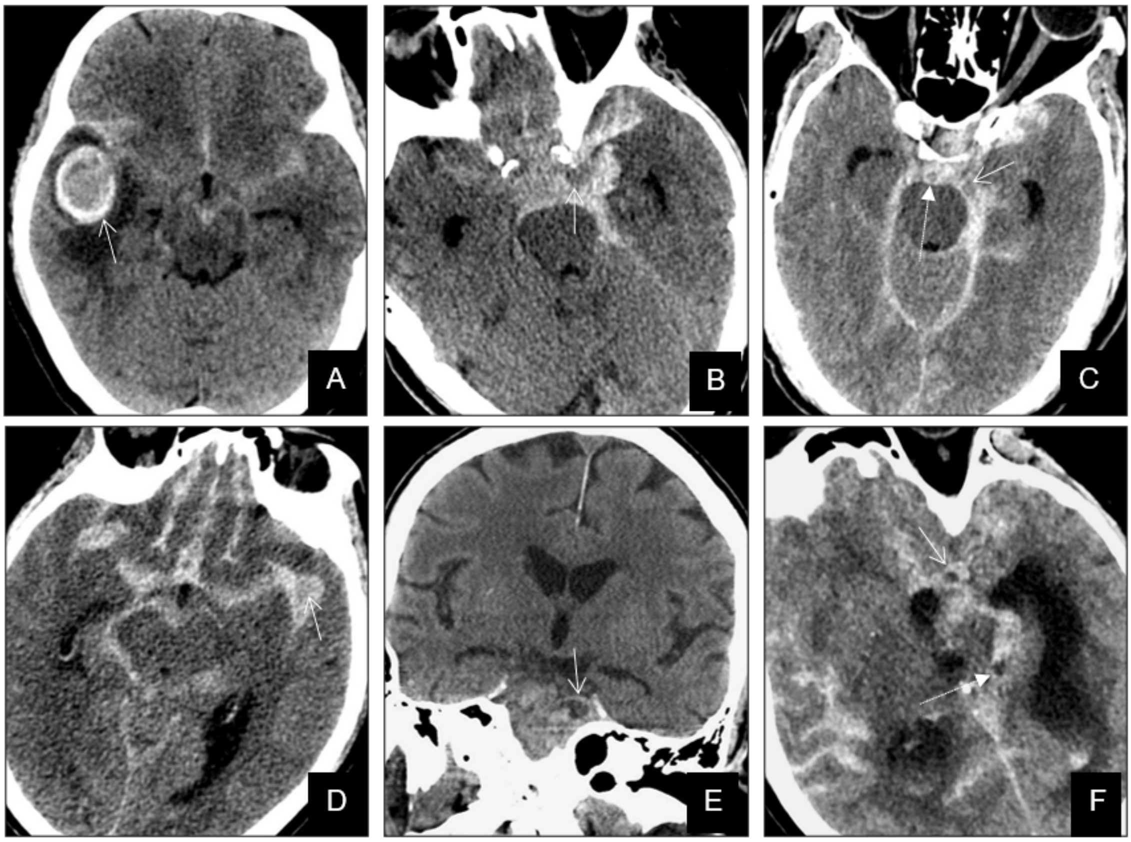

Figure 1: Illustration of hypo-attenuating berry sign (A–C) and its mimics (D–F) on non-enhanced brain computed tomography scan (NECT). A: Berry-shaped hypo-attenuating region in a patient with SAH (arrow). Note that there is an identifiable border between the hypo-attenuating berry sign and adjacent hemorrhage. B: Oval-shaped hypo-attenuating area was contained within the SAH and was not connected with the adjacent brain tissue (arrow). C: A small, round, isolated hypo-attenuating area with a sharp contrast between the hypo-attenuating region and adjacent hyper-attenuating SAH (arrow). The dotted arrow indicates the basilar artery. D: A relatively hypo-attenuating area with a vaguely defined margin between the hypo-attenuating area and adjacent SAH (arrow). E and F: A small, round, isolated hypo-attenuating region with a sharp border contained within SAH. The CT Hounsfield unit of hypo-attenuating region is similar to the value of cerebrospinal fluid (arrow and dotted arrow) and more than 1/4 length of the circumference of hypo-attenuating region connected with the adjacent brain tissue (dotted arrow).

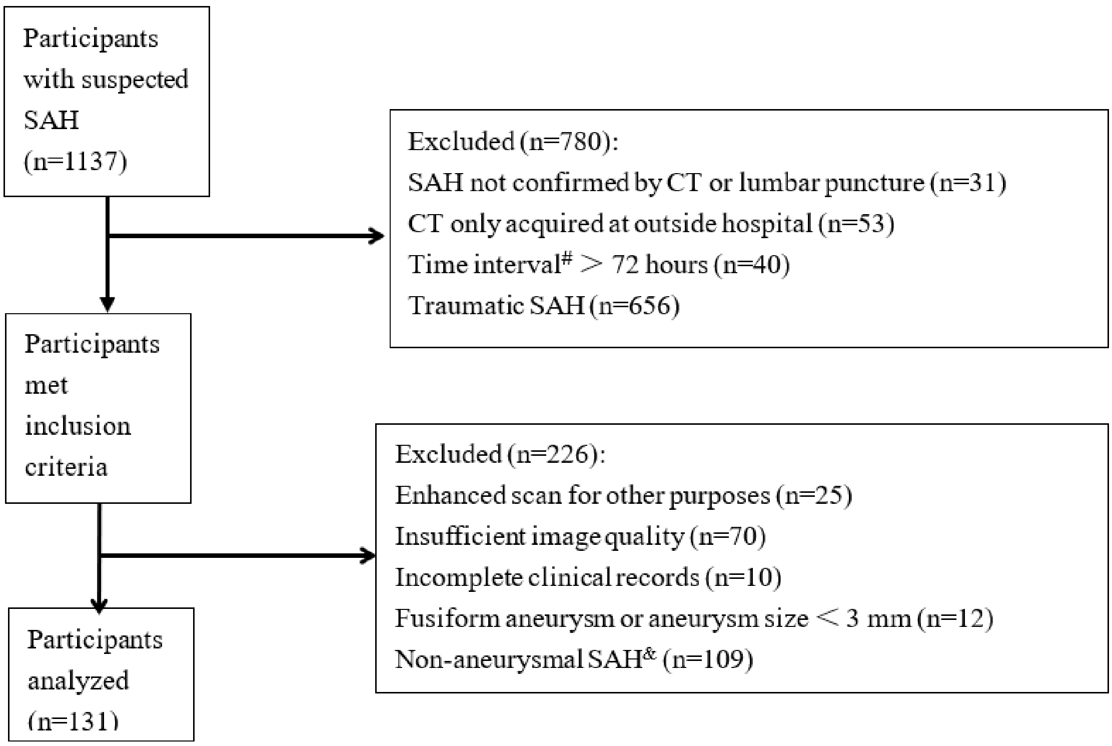

Figure 2: Flowchart of study case selection. #, time interval between non-contrast computed tomography (CT) scan and symptom onset; &: Non-aneurysmal subarachnoid hemorrhage (SAH) related to brain tumor, arteriovenous malformation, arteriovenous fistula, moyamoya disease, or hemorrhagic infarction.

Table 1: Clinical severity of subarachnoid hemorrhage (SAH) in studied cases based on Hunt-Hess and Fisher scores (n=131)

Scores	Number (%)
Hunt-Hess	
1	7 (5.3)
2	22 (16.8)
3	56 (42.7)
4	28 (21.4)
5	18 (13.7)
Fisher	
1	13 (9.9)
2	5 (3.8)
3	28 (21.4)
4	85 (64.9)

Table 2: Comparing the baseline characteristics between cases with and without Hypo-attenuating Berry Sign (HBS) by two readers

Variables	**HBS (Reader 1)**			**HBS (Reader 2)**		
	Positive (n=107)$^{\$}$	**Negative (n=44)$^{\$}$**	**P**	**Positive(n=108)$^{\$}$**	**Negative (n=40)$^{\$}$**	**P**
Age (year)						
Mean ± SD	61.9±10.1	62.8±11.9	0.651	61.6±10.1	63.7±12.2	0.289
Sex						
Female	67(62.6)	30(68.2)	0.517	69(63.9)	25(62.5)	0.206
Underlying conditions						
Diabetes mellitus	12(11.2)	10(22.7)	0.068	12(11.1)	10(25.0)	0.035
Hypertension	81(75.7)	35(79.5)	0.611	84(77.8)	31(77.5)	0.971
Hyperlipidemia	7(6.5)	4(9.1)	0.839	8(7.4)	3(7.5)	1.000
Smoking	4(3.7)	3(6.8)	0.416	3(2.8)	4(10.0)	0.161
Median SAH severity scores						
Hunt-Hess ≥ 3	91(85.0)	29(65.9)	**0.008**	93(86.1)	24(60.0)	**<0.001**
Fisher ≥ 4	80(74.8)	22(50.0)	**0.003**	78(72.2)	21(52.5)	**0.024**
Time interval$^{\#}$ (hour)						
Mean ± SD	11.0±18.3	11.3±14.9	0.930	11.2±17.7	11.5±17.2	0.931
The value of SAH surrounding HBS (HU)						
Mean ± SD	62.6±7.9	61.0±9.4	0.288	63.0±8.1	58.9±12.1	**0.017**
Aneurism size$^{\&}$ (mm)						
Mean ± SD	6.7±3.2	4.4±1.6	**<0.001**	6.7±3.2	4.4±1.5	**<0.001**
Aneurism location&						
ACA	26(26.0)	6(20.7)		29(28.2)	311.5)	
MCA	19(19.0)	4(13.8)	0.779	18(17.5)	5(19.2)	0.329
ICA	42(42.0)	15(51.7)		44(42.7)	13(50.0)	
Posterior circulation	13(13.0)	4(13.8)		12(11.7)	5(19.2)	

Data are presented as mean ± standard deviation (SD) or frequency (%). $:129 aneurysms were identified in the studied cases, and 14 (10.7%) patients had multiple aneurysms; &: Size and location based on digital subtraction angiography (DSA) or surgical results, #: time interval between non-contrast CT and symptom onset; ICA: internal carotid artery; MCA: middle cerebral artery; ACA: anterior cerebral artery (including anterior communicating artery); HU: Hounsfield Units; SAH: subarachnoid hemorrhage

Table 3: Predictive factors of Hypo-attenuating Berry Sign (HBS) presence based on multivariate analysis

Variables	**Reader 1**		**Reader 2**	
	OR (95%CI)	**P value**	**OR (95%CI)**	**P value**
Age	0.986(0.935-1.039)	0.601	0.958(0.906-1.013)	0.128
Sex	3.184(0.961-10.548)	0.058	2.274(0.672-7.699)	0.187
Diabetes	0.627(0.173-2.274)	0.478	0.637(0.171-2.367)	0.501
Attenuation value* (HU)	1.031(0.970-1.096)	0.331	1.028(0.959-1.102)	0.436
Hunt-Hess score ≥ 3	0.918(0.256-3.298)	0.896	0.343(0.090-1.302)	0.116
Fisher score ≥ 4	0.906(0.284-2.889)	0.868	1.421(0.389-5.186)	0.595
Aneurism size$^{\&}$	1.667(1.238-2.244)	<0.001	1.696(1.231-2.335)	0.001
Aneurism location$^{\&}$				
ACA	1.747(0.348-8.775)	0.498	5.997(0.959-37.514)	0.056
MCA	2.662(0.439-16.148)	0.287	2.218(0.396-12.411)	0.365
ICA	1.853(0.413-8.309)	0.420	3.334(0.711-15.642)	0.127
Posterior circulation	Reference		Reference	

&: Size and location based on DSA results; *: the value of subarachnoid hemorrhage (SAH) surrounding HBS; HU: Hounsfield unit; ICA: internal carotid artery; MCA: middle cerebral artery; ACA: anterior cerebral artery (including anterior communicating artery); OR: Odds ratio; CI: confidence interval.

Table 4: Screening performance characteristics of hypo-attenuating berry sign (HBS) in predicting the presence of ruptured aneurysm in patients with subarachnoid hemorrhage

Value	Sensitivity	Specificity	PPV	NPV	Kappa
Overall					
Reader1	77.5(69.2 - 84.2)	68.2(45.1 - 85.3)	93.5(86.5 - 97.1)	34.1(20.9 - 50.0)	0.734
Reader2	79.8(71.7 - 86.2)	73.7(48.6 - 89.9)	95.4(89.0 - 98.3)	35.0(21.1 - 51.7)	
Aneurysm size ≤ 5mm					
Reader1	63.5(50.4 - 75.0)	68.2(45.1 - 85.3)	85.1(71.1 - 93.3)	39.5(24.5 - 56.5)	0.703
Reader2	68.3(55.2 - 79.1)	73.7(48.6 - 89.9)	89.6(76.6 - 96.1)	41.2(25.1 - 59.2)	
Aneurysm size > 5mm					
Reader1	90.9(80.6 - 96.3)	68.2(45.1 - 85.3)	89.6(79.1- 95.3)	71.4(47.7 - 87.8)	1.000
Reader2	90.9(80.6 - 96.3)	73.7(48.6- 89.9)	92.3(82.2- 97.1)	70.0(45.7 - 87.2)	
Patient with single aneurysm					
Reader1	84.8(75.9 - 91.0)	71.4(47.7 - 87.8)	93.3(85.5 - 97.3)	50.0(31.7 - 68.3)	0.766
Reader2	87.9(79.4 - 93.3)	77.8(51.9 - 92.6)	95.6(88.5 - 98.6)	53.8(33.7 - 72.9)	
Ruptured aneurysm[&]					
Reader1	86.5(78.4 - 92.0)	83.3(57.7 - 95.6)	97.0(90.8 - 99.2)	50.0(31.7 - 68.3)	0.772
Reader2	88.3(80.5 - 93.4)	77.8(51.9 - 92.6)	96.1(89.7- 98.7)	51.9(32.4 - 70.8)	

[&]: Size and location based on DSA results; *: the value of subarachnoid hemorrhage (SAH) surrounding HBS; HU: Hounsfield unit; ICA: internal carotid artery; MCA: middle cerebral artery; ACA: anterior cerebral artery (including anterior communicating artery); OR: Odds ratio; CI: confidence interval.